Asociación Argentina
de Mecánica Computacional

Mecánica Computacional Vol XXVII, págs. 1999-2019 (artículo completo)
Alberto Cardona, Mario Storti, Carlos Zuppa. (Eds.)
San Luis, Argentina, 10-13 Noviembre 2008

EVALUATING THE EFFECT OF UNDERGROUND EXPLOSIONS ON STRUCTURES

Bibiana M. Luccioni[a,c] and Ricardo D. Ambrosini[b,c]

[a]*Instituto de Estructuras, Universidad Nacional de Tucumán, Av. Roca 1800, 4000 S.M. de Tucumán , Argentina, labest@herrera.unt.edu.ar.edu.ar , www.herrera.unt.edu.ar/iest*
[b] *Facultad de Ingeniería, Universidad Nacional de Cuyo*
Centro Universitario - Parque Gral. San Martín - 5500 Mendoza, dambrosini@uncu.edu.ar , http://fing.uncu.edu.ar/
[c]*CONICET, Av Rivadavia 1917, Cdad de Bs As*

Key words: Explosion, soil, blast wave, crater, damage, numerical model

Abstract.
During the last decades, research activity related to underground explosions and their effect on buried structures and structures located on or above ground level have progressively increased. The correct evaluation of the effect of this type of explosion is very important for the design of protection structures.
The action of buried explosions on soils and the resulting effect on structures is a strongly complex physical problem. The results are significantly dependent on many parameters that include the amount of explosive, the shape of the load, the explosion depth, soil type and properties, among others. Recent advances in numerical simulation have allowed the modeling of underground explosions. Although there are some papers related to this problem, the knowledge of the effect on buried structures or structures located on the ground is limited to a few numerical results without experimental validation or some isolated experimental observations.
The effect of underground explosions on buried structures or structures on or above soil surface is numerically studied in this paper. Numerical simulation is performed with a hydrocode. Different alternatives to model the soil are analyzed. The effect of soil model and parameters on blast wave propagation is particularly studied. In the case of structures located above the ground the capability of different numerical models to reproduce soil ejecta that impacts on structures is also studied.
The paper also compares the present numerical results with numerical values obtained by other authors using different hypothesis. Numerical results are contrasted with experimental results available in the specialized literature.

1 INTRODUCTION

Blasting loads have come into attention in recent years due to the great number of accidental or intentional events that affected important structures all over the world, clearly indicating that the issue is relevant for purposes of structural design and reliability analysis. In consequence, extensive research activities in the field of blast loads have taken place in the last decades (Alia and Souli, 2006; Ambrosini et al, 2002).

Much effort has been devoted to the study of underground explosions because they represent an actual risk. According to the 1999 Landmine Monitor report from the International Committee to Ban Landmines, estimates on the number of buried landmines worldwide range from 60 to 110 million (Cheeseman, 2006). Protective equipment, either for personnel or vehicles, must be designed to mitigate the effect of a landmine blast (Cheeseman, 2006; Gupta, 1999). As a result, there is a need for modelling and understanding the interaction of mine blast products with structures and the resulting loading and damage mechanisms inflicted by explosive blast and impact. This understanding is required both for damage assessment and protective hardening of both wheeled and tracked vehicles.

By the other side, underground reinforced concrete structures are used for essential installations protected against the effects of conventional weapons (Wang et al., 2005). The physical processes that govern the response of the underground structure are very complex, involving dynamic interactions among the explosive, the soil and the underground structure (Wang et al., 2005). Major phenomena include the formation of the crater or camouflet by the explosion; the propagation of the shock wave and elastic–plastic wave in the soil; and the interaction between soil and the structure.The high intensity, short term loading imparted by the explosion is enormously complex and can be significantly affected by a number of parameters including the size, shape, type, detonation point and depth of burial of the explosive and the type, density and water content of the soil (Cheeseman, 2006).

A number of studies have been performed in the general area of blast response of structures over the years. However, the loading mechanisms from explosive blast-soil-structure interaction such as those occurring from detonation of a buried mine below a vehicle are poorly understood at present. There are some numerical results obtained by different authors but experimental validation is still limited.

The destructive output of the PMN mine was assessed experimentally by detonating actual mines in air and then in soil by Swinton and Bergero (2004). The fragmentation pattern was recorded using a combination of flash X-rays, fragmentation packs, and gelatine cylinders. It was proved that soil has a strong influence on the characteristics of the fragmentation and blast produced by the mine.

Hlady (2004) demonstrated that the energy released by a mine varies greatly with the soil conditions surrounding it. Tests were conducted simulating a landmine in engineered soil containers: Different variables including standoff, explosive overburden, soil type, moisture, and density were studied.

Gupta (1999) modeled the mine-soil-structure interaction problem with a landmine buried in two different soil types using a hydrodynamic code. Two widely differing soil types: dry sand and fully saturated tuff, were studied. Considerable differences between the momentum transferred to a plate due to the detonation of explosive loads in both types of soil were found.

Recently Wang et al. (2003, 2004) have formulated a numerical three-phase soil model which is capable of simulating explosion and blast wave propagation in soils. Using this model, Lu et al. (2005) and Wang et al. (2005), performed fully coupled numerical model simulations of the response of a buried concrete structures under underground explosions. The

SPH (smooth particle hydrodynamics) technique was employed to model the explosive charge and the close-in zones where large deformation takes place, while the normal FEM is used to model the remaining soil region and the buried structure. A good agreement of numerical results with empirical predictions was found in both papers.

Cheeseman et al (2006) performed a coupled Eulerian-Lagrangian analysis to study the blast output of explosives buried in saturated sand. The explosive charge size, its depth of burial, the target stand-off, the distance and the dimensions of the target plate were varied and the accuracy of the numerical simulations when compared with the experimental observations was discussed.

Elgy et al. (2006) describes a series of numerical simulations in which the effect of detonating an explosive within a matrix of particles, and the subsequent blast and particulate interaction with a target, was simulated. The momentum transferred is investigated as a function of the technique used to model fragmentation and detonation proximity.

A new materials model for sand has been developed by Grujicic et al.(2006) in order to include the effects of the degree of saturation and the deformation rate on the constitutive response of this material. This material model for sand was used, within a non-linear-dynamics transient computational analysis, to study various phenomena associated with the explosion of shallow-buried and ground-laid mines. The computational results were compared with the corresponding experimental results obtained through the use of an instrumented horizontal mine-impulse pendulum, pressure transducers buried in sand and a post-detonation metrological study of the sand craters.

Experimental results for the mechanical response of sand (at different levels of saturation with water) under shock-loading conditions were recently used by Grujicic et al. (2008) to parameterize their new material model for sand (Grujicic et al 2006). The model was used to simulate the detonation of a landmine buried in sand and the interactions of the detonation products, mine fragments and sand ejecta with various targets.

The authors of the present paper have conducted a series of tests performed with different amounts of explosive at short distances above and below ground level, as well as on the soil surface (Ambrosini et al., 2002). They also presented (Ambrosini and Luccioni, 2006) a numerical study on craters formed by explosive loads located on the soil surface. The soil parameters used in the numerical model, as well as the analysis procedure, were validated against experimental observations of the crater diameters. Moreover, the effect of elevation of the centre of energy release of explosive loads located on the soil surface were analyzed and discussed. Simple predictive equations for the crater diameter were presented.

In a recent paper, the accuracy of numerical simulations of craters produced by underground explosions was proved (Luccioni and Ambrosini, 2006). For this purpose, the numerical analysis of crater formation due to underground explosions was performed with a hydrocode. Several numerical approaches were carried out using different models and processors for the soil. Moreover, different alternatives for the constitutive model of the soil were used. In order to validate the numerical approach and prove its ability to model the crater formation, comparison with experimental results is performed. Many simulations of the same physical model lead to the same crater dimensions and a good agreement between the test results and the predicted crater measures was achieved.

It was proved in both papers (Luccioni and Ambrosini, 2006; Ambrosini and Luccioni, 2006) that the elastic properties of the soil do not significantly affect the diameter of the crater obtained. It was also demonstrated that the diameter of the final remains unchanged when the failure limit and the yield function are changed between reasonable limits.

The authors have also analyzed the blast wave propagation through soil and the effect on

objects located over the ground is analyzed in a previous paper (Luccioni and Ambrosini, 2007). Numerical results were compared with empirical and numerical results found in the literature. Numerical results for the propagation of blast wave in soils are coincident with those suggested by codes and obtained by other authors. They are strongly dependent on the type of soil modeled. Consequently, in order to assess the effect of buried explosions on underground structures, the soil properties and model should be more carefully studied and defined. For this purpose, underground structures should be explicitly modeled. The differences observed in reflected pressure values could be attributed to the simplicity of the model used in this paper, in which the underground structure was not actually modeled.

The effect of underground explosions on objects placed over the ground level also depends on soil properties. The influence of soil properties is practically negligible for null overburden but increases with the overburden of the explosive load. The results obtained for the soil models analyzed are comparable to experimental results for small overburdens, up to 100mm. Considerable difference between numerical and experimental results is obtained for the highest overburden analyzed. This difference could be attributed not only to the soil model but also to the Euler multi-material processor used for the soil. The Euler processor is not able to reproduce the actual soil ejecta.

Further numerical research, including soil model in the area of underground explosions and their effect on buried and over ground structures, is presented in this paper.

2 NUMERICAL SIMULATIONS

2.1 Introduction

All the numerical analysis is performed with a hydrocode (AUTODYN v11.0, 2007).

In order to carry out a comparable analysis, the mass of the explosive is defined by TNT masses. The corresponding masses for other explosives can be obtained through the concept of TNT equivalence (Formby, 1996).

An n Euler Godunov multi material with strength higher order processor (Alia and Souli, 2006) is used to model the problems including the air, the explosive charge and the soil. Solids like steel plates and concrete pavement are modeled using Lagrange processor.

2.2 Material models

2.2.1 Air

The ideal gas equation of state is used for the air. In an ideal gas, the internal energy is a function of the temperature alone and if the gas is polytropic the internal energy is simply proportional to temperature. It follows that the equation of state for a gas, which has uniform initial conditions, may be written as,

$$p = (\gamma - 1)\rho e \tag{1}$$

in which p is the hydrostatic pressure, ρ is the density and e is the specific internal energy. γ is the adiabatic exponent, it is a constant (equal to $1 + R/c_v$) where constant R may be taken to be the universal gas constant R_0 divided by the effective molecular weight of the particular gas and c_v is the specific heat at constant volume. The values of the constants used for air are presented in Table 1.

Equation of State: Ideal gas
$\gamma = 1.4$
Reference density: $\rho_a = 1.225\ 10^{-3}$ g/cm^3
Reference temperature: $T_o = 288.2$ K
Specific heat: $c_v = 717.3$ J/kgK

Table 1: Air properties

2.2.2. TNT

Lee-Tarver equation of state (Lee and Tarver, 1980) is used to model both the detonation and expansion of TNT in conjunction with "Jones - Wilkins - Lee" (JWL EOS) to model the unreacted explosive.

The (JWL) equation of state can be written as,

$$p = C_1\left(1-\frac{\omega}{r_1 v}\right)e^{-r_1 v} + C_2\left(1-\frac{\omega}{r_2 v}\right)e^{-r_2 v} + \frac{\omega e}{v} \tag{2}$$

where p is the hydrostatic pressure, $v = 1/\rho$ is the specific volume, ρ is the density, C_1, r_1, C_2, r_2 and ω (adiabatic constant) are constants and their values have been determined from dynamic experiments and are available in the literature for many common explosives. The values used for TNT are presented in Table 2.

Equation of State: JWL
Reference density $\rho = 1.658$ g/cm^3
$C_1 = 3.7377\ 10^8$ kPa
$C_2 = 3.73471\ 10^6$ kPa
$R_1 = 4.15$
$R_2 = 0.9$
$\omega = 0.35$
C-J detonation velocity: $6.93\ 10^3$ m/s
C-J energy/unit volumen: $6\ 10^6$ KJ/m^3
C-J pressure: $2.1\ 10^7$ kPa

Table 2: TNT properties

2.2.3. Soil

In order to study the influence of the soil model and soil properties, the four types of soil described in the following lines are defined.

A linear equation of state combined with elastoplastic strength model are used for Soils 1 and 2 that only differ in their elastic constants. Properties of: Soil 1 and Soil 2 defined in Table 3, are considered.

Equation of State: Linear	Strength: Drucker Prager
Reference density ρ = 2.2 g/cm^3	
Bulk Modulus K	K_1= 2.2 10^5 kPa K_2= 3.52 10^5 kPa
Shear Modulus G	G_a= 1.5 10^5 kPa G_2= 2.4 10^5 kPa
Pressure 1 =-1.149 10^3 kPa	Yield stress 1 = 0 kPa
Pressure 2 = 6.88 10^3 kPa	Yield stress 2 = 6.2 10^3 kPa
Pressure 3 = 1.0 10^{10} kPa	Yield stress 3 = 6.2 10^3 kPa
Hydro tensile limit p_{min} = -100 kPa	

Table 3: Soil1 and Soil2 properties

A shock equation of state combined with an elastoplastic strength model based on Drucker Prager criterion and a hydro tensile limit are used for the soil3. The initial density is taken as ρ = 2.2 g/cm3 (wet density). The wet density is obtained considering a mean dry density of 2100 kg/m3 and a moisture content of 5%.

The experimental fact is that for most solids and many liquids, that do not undergo a phase change, the values on the shock Hugoniot for shock velocity U and material velocity behind the shock u_p can be adequately fitted to a straight line

$$U = c_o + s u_p \tag{3}$$

where c_0 is sound speed.

The Mie-Gruneisen form of equation of state based on the shock Hugoniot is used:

$$p = p_h + \Gamma\rho(e - e_h) \tag{4}$$

where Γ is the Gruneisen Gamma G, defined as:

$$\Gamma = v\left(\frac{\partial p}{\partial v}\right)_v \tag{5}$$

It is assumed that $\Gamma\rho = \Gamma_0\,\rho_0 = constant$ and

$$p_h = \frac{\rho_o c_o^2 \mu(1+\mu)}{[1-(s-1)\mu]^2} \qquad e_h = \frac{1}{2}\frac{p_h}{p_o}\left(\frac{\mu}{1+\mu}\right) \tag{6}$$

The assumption of constant $\Gamma\rho$ is probably not valid. Furthermore the assumption of a linear variation between the shock velocity U and the particle velocity u_p does not hold for too large a compression. At high shock strengths some nonlinearity in this relationship is apparent, particularly for non-metallic materials. This non linearity is covered by a smooth interpolation between two linear relationships.

A Drucker Prager criterion with standard values is adopted for the strength model. The yield stress is a piecewise linear function of pressure.

A summary of soil properties used for soil3 is presented in Table 4.

Equation of State: Shock	Strength: Drucker Prager
Reference density $\rho = 2.2$ g/cm^3	
Gruneisen Gamma $\Gamma = 0.11$	
$c_o = 1.614\ 10^3$ m/s	
$S = 1.5$	
Shear Modulus $G = 2.4\ 10^5$ kPa	
Pressure 1 =-1.149 10^3 kPa	Yield stress 1 = 0 kPa
Pressure 2 = 6.88 10^3 kPa	Yield stress 2 = 6.2 10^3 kPa
Pressure 3 = 1.0 10^{10} kPa	Yield stress 3 = 6.2 10^3 kPa
Hydro tensile limit p_{min} = -100 kPa	

Table 4: Soil 3 properties

A compaction equation of state combined with a MO granular strength model is used for Soil 4 that represents a dry sand.

Compaction equation of state is an extension of the Porous equation of state that allows more control over loading/unloading slopes.

In linear porous Equation of state the plastic compaction path is defined as a piecewise linear function from which unloading and reloading can occur along an elastic line.

Using this model, a material initially compacts from $\rho = \rho_o$ along an elastic path defined by the differential equation

$$\frac{dp}{d\rho} = c_{init}^{\ 2} \tag{7}$$

until the pressure reaches the plastic yield stress defined by the value of the pressure in the first (ρ , p) pairs. Subsequent loading takes place along the plastic compaction path until the material is fully compacted, at which time further compression takes place according to the linear relationship

$$p = c_s^2(\rho - \rho_{ref}) \tag{8}$$

As the material compacts, elastic / unloading uses a bulk sound speed interpolated between c_{por} bulk sound speed of the porous material) and c_s (bulk sound speed of the solid, fully compacted material)

$$c_{\text{int}} = c_{por} + (c_s - c_{por})\left(\frac{\alpha - \alpha_1}{1 - \alpha_1}\right) \tag{9}$$

where

$\alpha = \rho_{ref} / \rho$ is current porosity (porosity is the reciprocal of compaction)

$\alpha_1 = \rho_{ref} / \rho_1$ is the starting porosity

and the path is always computed from the differential equation (7).

In the compaction model, instead of being linearly interpolated between density values of the fully porous and fully compacted states, the elastic sound speed is defined as a piecewise-linear function of density.

MO Granular Model is an extension of the Drucker-Prager model that takes into account effects associated with granular materials. In addition to pressure hardening, the model also models density hardening and variations in the shear modulus.

Material properties for Soil 4 are consigned in Table 5.

Equation of State: Shock Compaction				Strength MO granular			
Reference density ρ = 2.641 g/cm3							
Pressure (kPa)	Density (g/cm^3)	Soundspeed (m/s)	Density (g/cm^3)	Pressure (kPa)	Strength (kPa)	Density (g/cm^3)	Shear Mod. (kPa)
0.000	1.674	2.652E+02	1.674	0.000	0.00E+0	1.674	7.69E+4
4.577E+03	1.739	8.521E+02	1.745	3.40E+3	4.23E+3	1.746	8.69E+5
1.498E+04	1.874	1.722E+03	2.086	3.49E+4	4.47E+4	2.086	4.03E+6
2.915E+04	1.997	1.875E+03	2.147	1.01E+5	1.24E+5	2.147	4.91E+6
5.917E+04	2.144	2.265E+03	2.300	1.85E+5	2.26E+5	2.300	7.77E+6
9.809E+04	2.250	2.956E+03	2.572	5.00E+5	2.26E+5	2.572	1.48E+7
1.794E+05	2.380	3.112E+03	2.598	Hydro tensile limit p_{min} = -100 kPa		2.598	1.66E+7
2.894E+05	2.485	4.600E+03	2.635			2.635	3.67E+7
4.502E+05	2.585	4.634E+03	2.641			2.641	3.73E+7
6.507E+05	2.671	4.634E+03	2.800			2.800	3.73E+7

Table 5: Soil 4 properties

2.2.3 Steel and Concrete

In the examples, steel and concrete structures are modeled using standard models for this types of materials. An elastoplastic model is used for steel and RHT model is used for concrete. The models are not described in present paper because they play a secondary role for the results presented.

2.2.4. Erosion

In the case of concrete elements an erosion criteria is used together with the models described. Erosion is used to remove Lagrange cells from the calculation when they are too distorted. When a cell is removed from the calculation process in this way, the mass within the cell is distributed to the corner nodes of the cell.

An instantaneous geometric strain limit is used as erosion criteria in this paper. The value of this strain is studied in each example. It is important to note that, in general, this is not true modeling of a physical phenomena but a numerical tool introduced to overcome the problems associated with the mesh distortions caused by gross motions of a Lagrangian grid.

2.3 Boundary conditions

In order to fulfill the radiation condition, a transmitting boundary is defined for soil subgrids external limits. The transmit boundary condition allows a stress wave to continue "through" the physical boundary of the subgrid without reflection. The size of the numerical mesh can be reduced using this type of boundary condition. The transmit boundary is only active for flow out of a grid. The effectiveness of this boundary condition is checked in some of the examples presented in this paper.

Flow out of air and TNT is also allowed in all external limits of air mesh.

3 SOIL EJECTA

The tests performed by Swinton and Bergeron (2004) are reproduced in this section. A steel container 800 mm in diameter and 500 mm deep was filled with dry medium sand. The mines were buried at the centre of the container such that the top was 20 mm below the surface. A total of five tests were performed with buried mines. Three of these tests used PMN mines with a 240 g of TNT fill, while the other two tests were performed with PMN mine bodies that had been refilled with 200 grams of PE4

Figure 1, taken from Swinton and Bergeron (2004) presents six radiographs of the expanding detonation products. I takes between 30 and 50 μs, before any motion of the soil is visible. The soil cap then rises, taking a hemispherical shape. Radiographs show a region of high density directly above the mine. The soil was compressed into a .solid cap. that broke up soon thereafter. The vertical position of the front of detonation products/soil ejecta was measured and the velocity was determined.

The model used to simulate these blast experiments is presented in Fig.2. Although the complete model is shown, due to symmetry of the problem, it was solved with and axial symmetric model. A total of 200x300 elements were used. Cells dimension were refined in the centre of the model where 2mmx2mm elements were used. The complete problem was modelled with an Euler Multi Material processor.

In order to represent the steel container, soil was not allowed to flow in soil limits, while flow out of air was allowed in the upper part of the model.

The four different models described in section 2 were used to model the soil. Fig. 4 shows the soil ejecta numerically obtained with soil1 for the same time instants than those presented in Figure 2. It can be seen that the shape of the cap emerging from the soil is similar to that observed in the tests presented in Fig. 2.

In order to compare the ability of different soil models to reproduce this problem, the vertical displacements and velocity of the top of soil ejecta are recorded for soils 1 to 4 and they are presented in Table 6 compared with experimental results. From Table 6, it could be concluded that this sand can be approximately modelled by soil1 or soil2 that approximately reproduce the vertical displacement and velocity of soil ejecta.

The problem was also solved with a more dense mesh where the size of the elements was reduced to half the size in the first model. Identical results were obtained for this latest model.

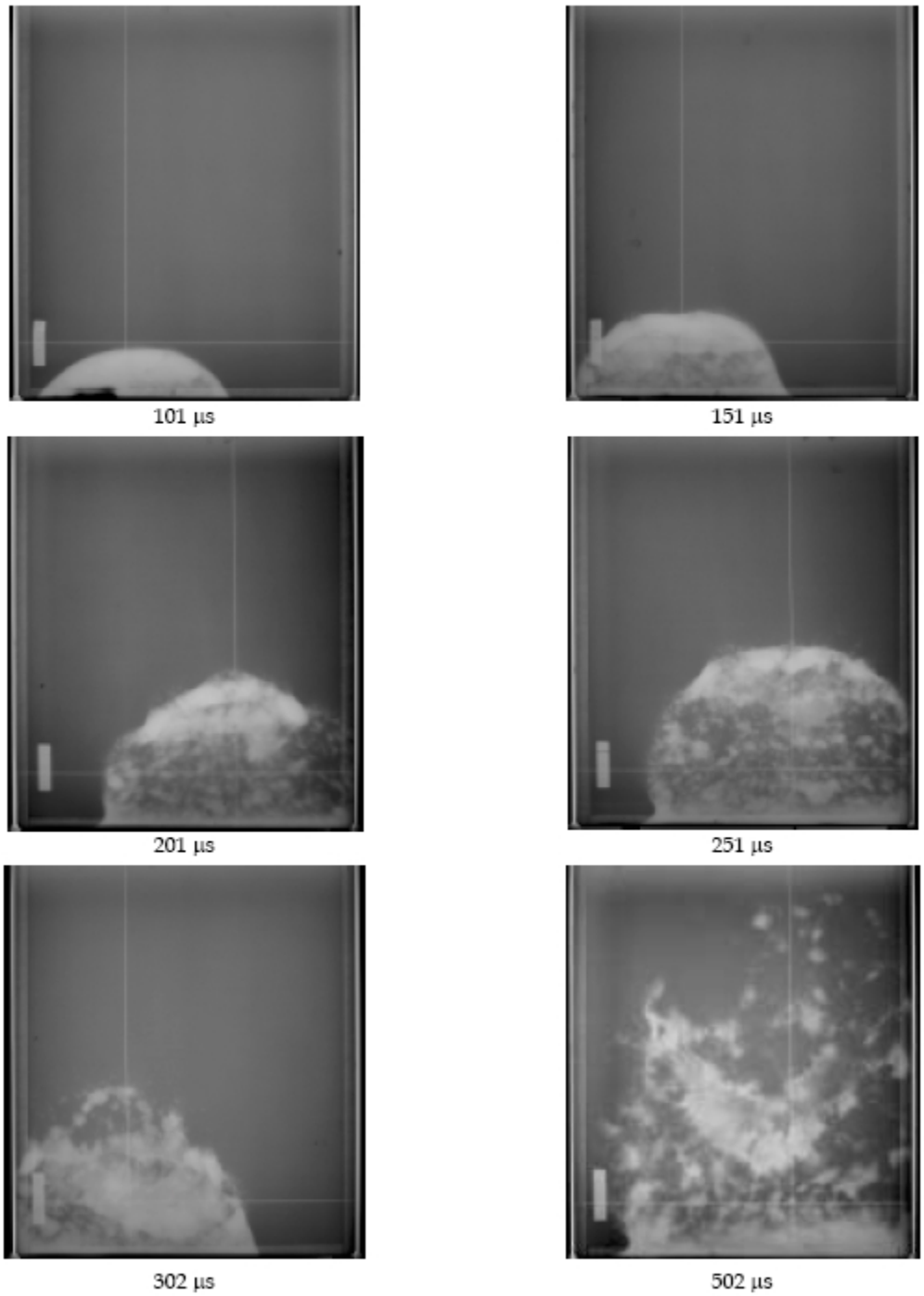

Fig1. Expansion of the detonation products and soil ejecta (Swinton and Bergeron, 2004)

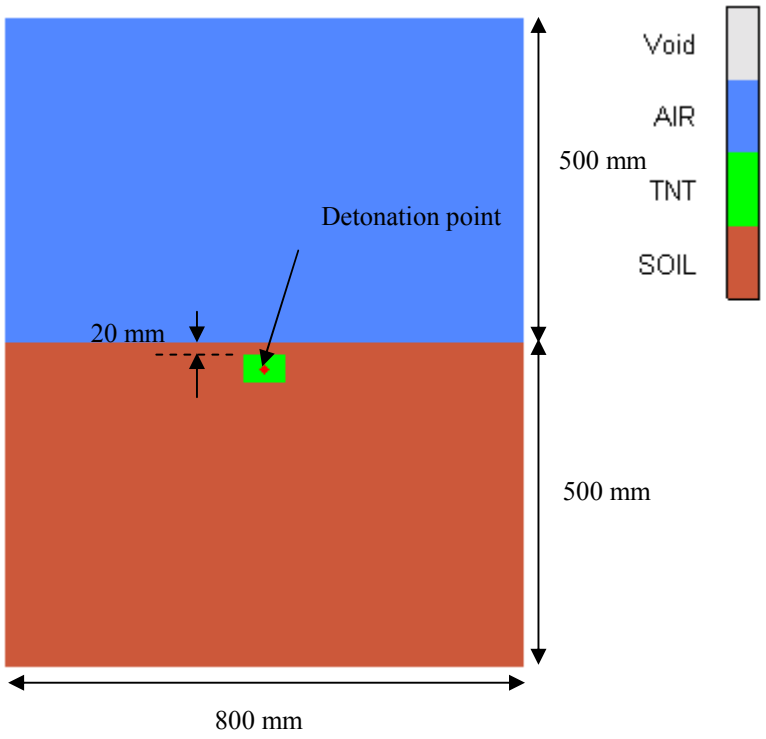

Fig.3.Numerical model used to simulate Swinton and Bergeron (2004) blast tests

Time (ms)	Displacement (mm)					Velocity (m/s)				
	Soil1	Soil 2	Soil3	Soil4	Exper,	Soil1	Soil 2	Soil3	Soil4	Exper,
0.101	76	78	100	98	80	963	971	1071	1207	
0.151	125	125	153	159	110	986	977	1161	1209	820
0201	172	172	206	219	175	1001	1015	1166	1182	to
0.251	219	219	263	279	195	928	1003	1171	1158	926
0.302	258	268	321	334	---	954	1061	1027	1138	

Table 6: Vertical displacement and velocities obtained for different types of soils

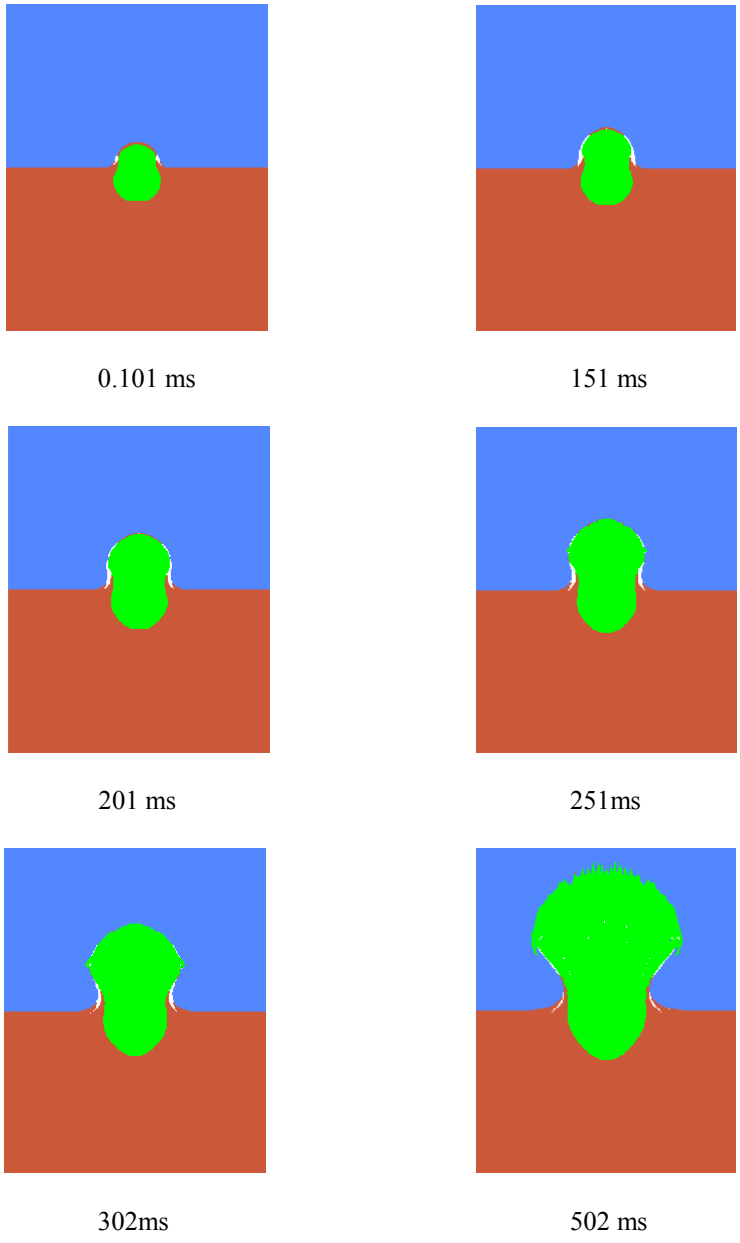

Fig.4 Numerical simulation of detonation products expansion

4 BLAST PROPAGATION AND EFFECT ON BURIED STRUCTURES

The propagation of the blast wave produced by underground explosions in soils and the effect on underground structures was analyzed by Luccioni and Ambrosini (2007). For this purpose, the numerical tests performed by Lu et al. (2005) were numerically reproduced. A good agreement of peak pressure attenuation with scaled distance with the values suggested by TM5-855-1 (1984) was achieved when soil1 was used.

The effect on a buried reinforced concrete structure is simulated in this paper.

The model is presented in Figure 5. Explosive load is coincident with point 1. Air, soil and the explosive load are simulated with an Euler multimaterial processor while a Lagrange processor is used for the reinforced concrete structure. A RHT model with an instantaneous geometric strain erosion limit of 0.01 is used for concrete. Interaction between Euler and

Lagrange meshes is activated.

Gauges points are indicated in Fig. 5.The reflected pressure time history for points 8 to 10 located on the structure front face are shown in Fig.6. The curves show multiple reflections of the blast wave on the concrete structure. The maximum peak reflected pressure value obtained for Point8 and is greater than that obtained in a previous work (Luccioni and Ambrosini 2007) assuming a rigid border. The mean value on the structure face is similar to that reported by reported by Lu et al. (2005) for the peak pressure acting on a concrete structure placed at 10m from the explosive charge.

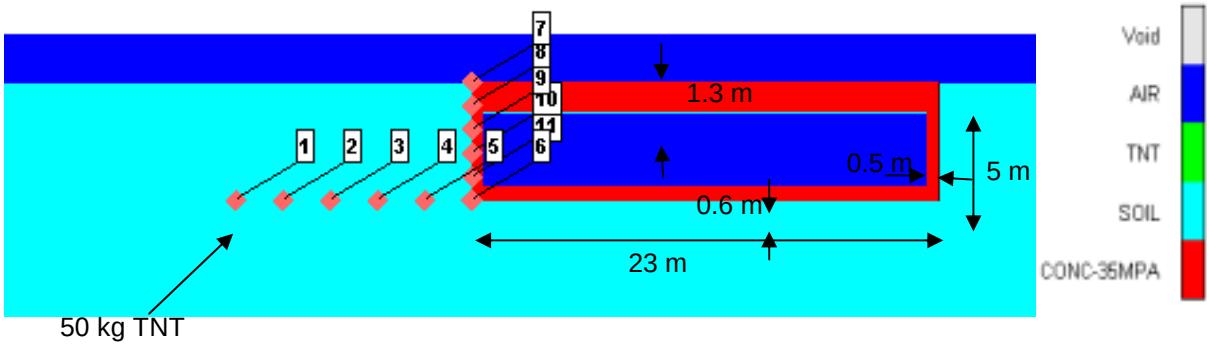

Figure 5. Effect of 50 kg of TNT on a buried structure. Problem Setup

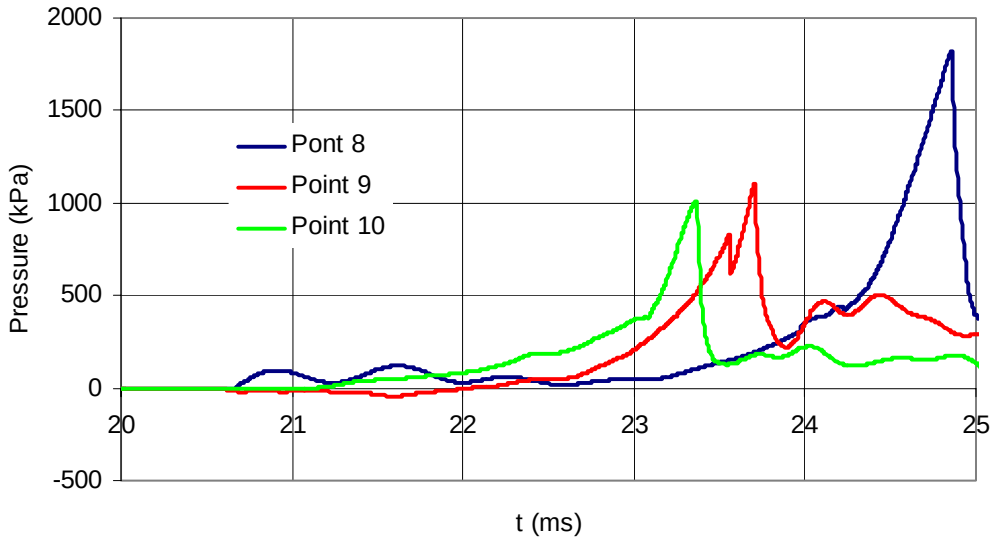

Figure 6. Pressures Histories

5 EFFECT ON STRUCTURES ON THE SOIL SURFACE

The detonation of a spherical TNT charge of 100 kg of TNT placed at 74 cm depth (Wang et al., 2005) was analyzed in a previous paper (Luccioni and Ambrosini 2007).. A good agreement with experimental and previous numerical results for the crater diameter was obtained. The blast wave propagation in soil was also studied and it was found that the velocity values are strongly dependent on soil model and material properties. A good

agreement with numerical results was obtained when soil 1 was used.

The same problem is solved in this paper but a concrete pavement is added on the soil surface. Figure 7 shows the model setup for this problem. Actually, only half of the problem was model because the axial symmetry. A Lagrange processor was used for the pavement and the rest of the problem was modelled with an Euler multimaterial processor.

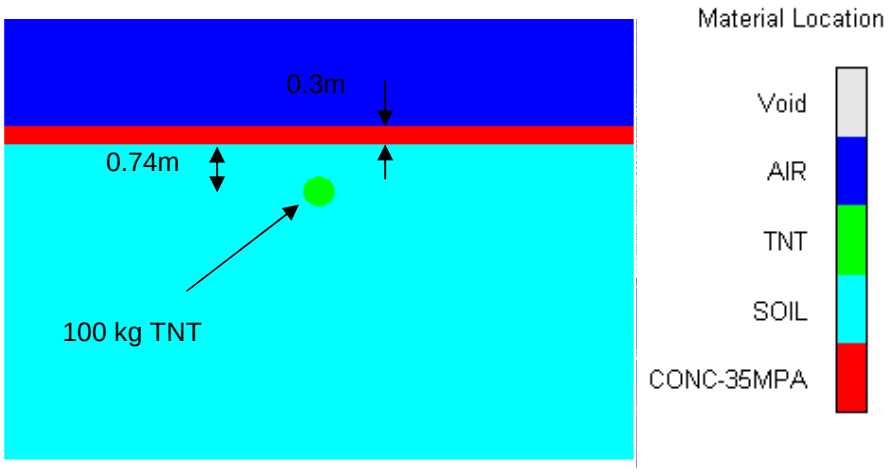

Figure 7. Effect of a buried explosion (100 kg of TNT) on a concrete pavement. Problem Setup

RTH model was used for the pavement concrete. Different values of the erosion limit were proved in order to obtain the maximum value (0.001) for which overlapping faces are prevented.

The problem was solved for different mesh sizes and similar results were always obtained.

Fig. 8 shows the crater obtained for an erosion limit of 0.001. The diameter of the soil crater (5.40m) has been reduced form the original for no pavement (7.24m).The diameter of the pavement crater obtained is 6.66 m. The size of the crater is now strongly dependent on the erosion limit used for concrete. Velocity values below the ground level are also altered by the presence of the pavement that represents a reflecting surface for the soil. The velocity time histories for different gauges points are presented in Fig. 9

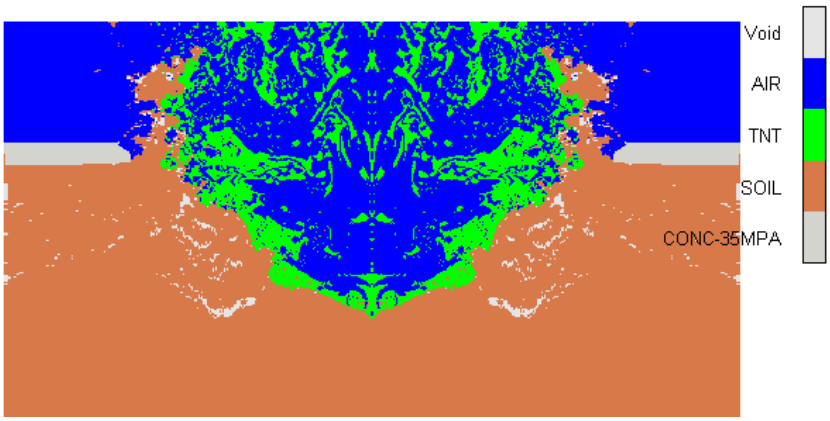

Figure 8. Crater produced by a buried explosion (100 kg of TNT) on a concrete pavement.

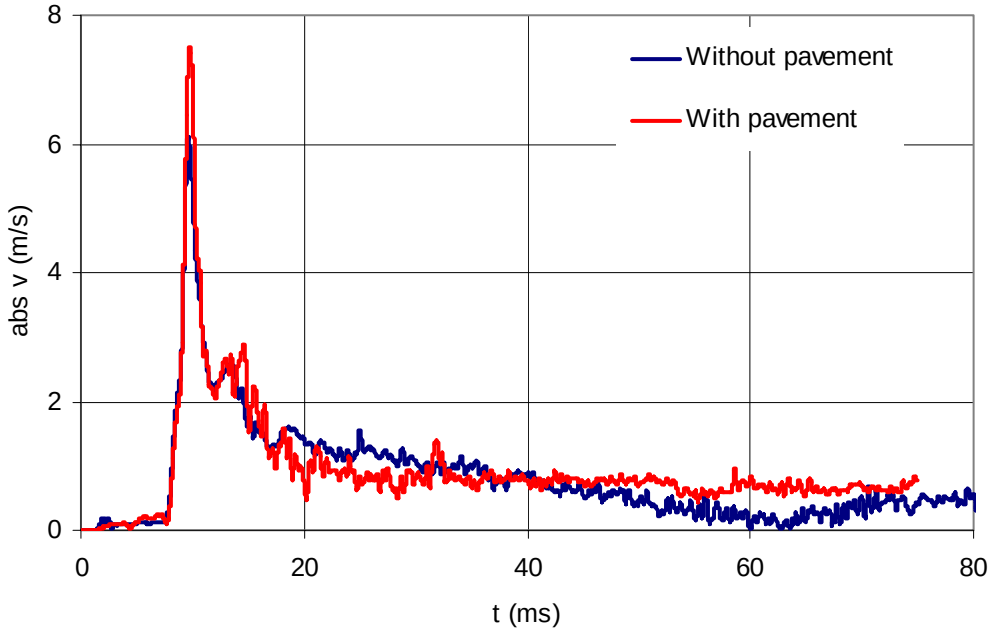

Figure 9. Velocity time-histories in soil

6 EFFECT ON STEEL PLATES OVER THE GROUND

6.1 Tests by Hlady (2004)

Hlady (2004) conducted a series of tests that consists on the explosion of landmines in soil containers with a target attached to a piston apparatus, mounted above the soil container. Energy transferred to the target was calculated from the height the piston jumped after the landmine was detonated. Variables included standoff, overburden, soil type, moisture, and density. High density, high moisture soil conditions produced seven times the energy transfer versus dry sand conditions. The target plate is 25.4 mm thick and 254 mm in diameter. The total mass of the target plate, mounting plate and shaft is 47 kg. Steel soil containers filled with different soils with different moisture contents were used.

For all trials, the landmine was 25g of C4, encased in plastic, with a height-to diameter ratio of 35%. Different overburdens from 0 to 150 mm were tested. Held (2002a) has done extensive research mapping the momentum distribution of AT landmines in sand. Most of the damage results from momentum transfer from the sand to the target (Held, 2002b). Therefore the ejecta is a significant source for the energy transfer to the target. When there is little or no overburden, the ejecta, and thus the energy transfer to the target, is reduced. Conversely, for large overburden, the soil is able to absorb a large amount of the explosive energy, and thus the amount of ejecta is reduced (in the extreme, an explosive buried deep underground does not produce any ejecta at all). Thus, there exists an optimum overburden for energy transfer. The trend observed by Hlady (2004) indicates an optimum overburden, for 25 g of C4, in CFAS, to be about 50 mm.

The tests performed by Hlady (2004) were numerically reproduced in a previous work

(Luccioni and Ambrosini 2007) using soil1 and soil2. These type of soil modeled gave values of energy transfer similar to those reported by Hlady (2004) for null overburden ($h_o = 0$). It is ease to show that, for this case, the value of the energy transfer to the target plate is practically independent on soil properties. For greater overburdens soil1 that is stiffer, transmits more energy to the plate. The values of energy transferred to the target plate numerically obtained for low overburdens, up to 100 mm were in the range of experimental results Hlady (2004). But for $h_o = 150mm$, numerical results are strongly higher than obtained experimental results, indicating the need of further numerical research.

The same problem is solved in this paper for soil4 in order to analyze the effect of soil model on the numerical results. The numerical model used for this problem is presented in Figure 10. As the problem presents axial symmetry a 2D model is used. The soil, the air and the explosive are simulated with the same models and processors than in the other examples.

Taking into account that the TNT equivalence of C4 is 1.078 (TM5-855-1, 1984), $W_{TNTequiv} = 1.078\ \ 25\text{g} = 26.95g$ of TNT are used as explosive charge instead of a 25g of C4 actually used in the tests.

Only a 400 mm diameter and 270 mm height soil cylinder is modeled. This cylinder represents the central upper part of the soil container. In order to represent the rest of the soil surrounding this part, transmit boundaries conditions are assigned to the lateral and bottom surfaces of the soil cylinder. The target plate is model with a 254 mm diameter plate. The thickness of this plate is increased (118.4 mm) to represent the total mass of the target plate, the mounting plate and the shaft. The plate is solved with a Lagrange processor. Euler Lagrange interaction is defined to take into account the interaction of air, explosive and soil with the steel plate.

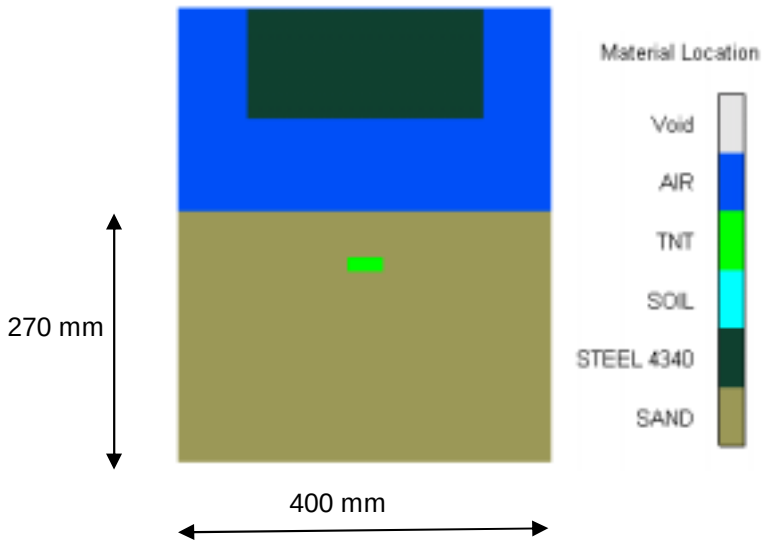

Figure 10. Numerical Model (50 mm overburden)

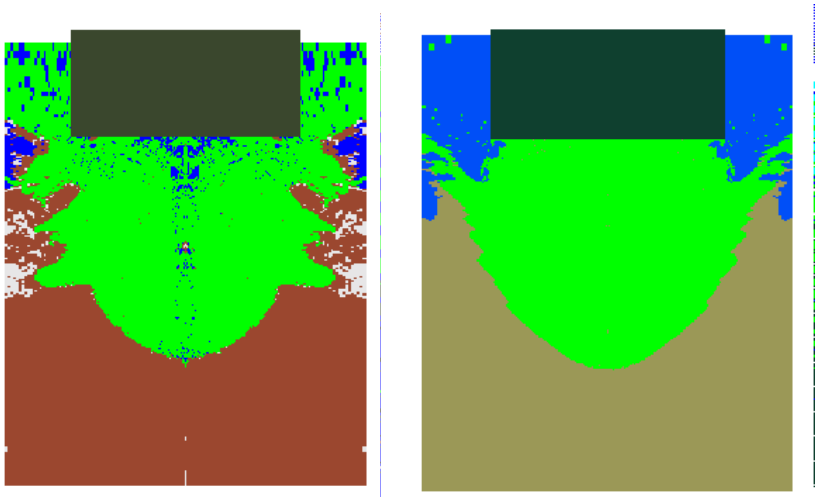

a) b)

Figure 11. Comparison of craters and soil ejecta for different types of soil. A) Soil1, b) Soil4

Figure 11 shows the soil ejecta previously obtained by Luccioni and Ambrosini (2007) for soil1 and the comparison with soil ejecta obtained for soil4 in the present paper. Both imagines correspond approximately to the same time instant and, although the diameter of the caters are similar, the shapes of soil ejecta are strongly different. A notable difference is also obtained for the values of the energy transfer to the steel plate that are sensible lower than those previously obtained for soil1 and soil2. The results for overburdens from 0to 150 mm are ploted in Figure 12 together with experimental results and previous numerical results in Luccioni and Ambrosini (2007). It is clear that soil4 (sand) can better approximate the experimental behavior reported by Hlady (2004).

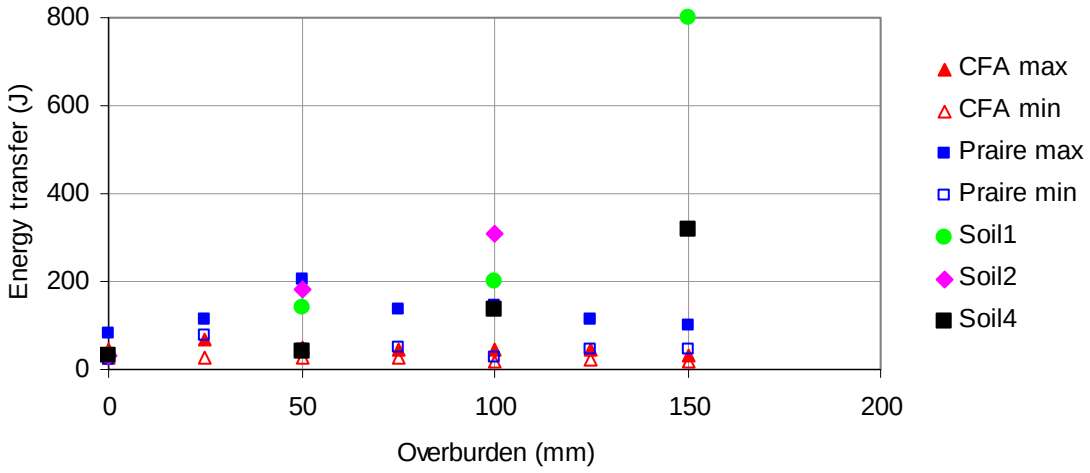

Figure 12. Energy Transfer to the Target Plate for Different Overburdens

6.2 Numerical tests by Gupta (1999)

The problem analyzed by Gupta (1999) involves the worst-case scenario of a shallow-buried cylindrical mine embedded all around in two different soil types: dry sand and wet soil

with a 15-cm soil overburden. The mine contains explosive with an equivalent charge weight of 10 kg TNT and is asymmetrically located with a horizontal centerline offset distance of 61 cm relative to a square plate 244 cm x244 cm. Plate thicknesses of 15 cm and 20 cm were modeled. The vertical standoff between the bottom plate surface and the top of the soil overburden was 41 cm. The cylindrical mine has a diameter of 32 cm and a height of 9 cm and was located inside a block of soil 366 cm in diameter with a total height of 124 cm.

The model used to simulate this problem in the present paper is shown in Figure 13. Although the problem is three-dimensional, plain strain condition was assumed as simplification. In order to reproduce the same case than Gupta (1999), the soil block and the steel plate were placed in a bigger air mesh. Both soil and air were modeled with an Euler multimaterial processor while Lagrange processor was used for the plate. In order to analyze the influence of soil model on the results and to verify the ability of soil models to reproduce the behavior of different kinds of soils, the problem was solved for different soil models.

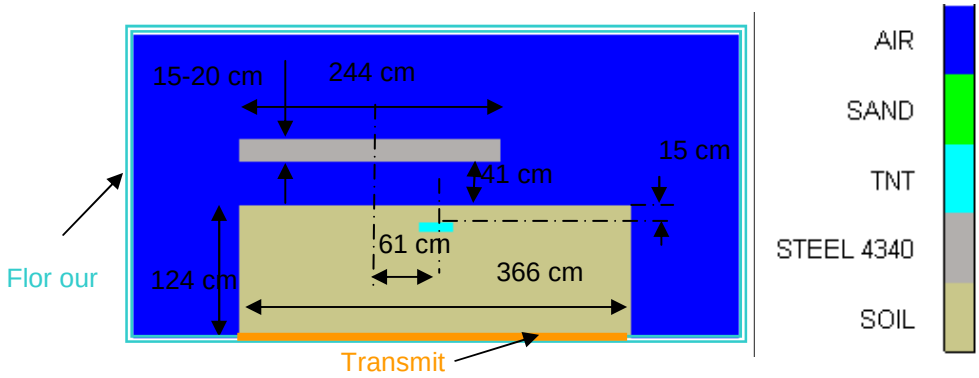

Figure 13. Cylindrical landmine below a steel plate. Problem setup.

The soil ejecta and the position of the steel plate 8ms after the detonation of the mine in soil1 can be observed in Figure 14.

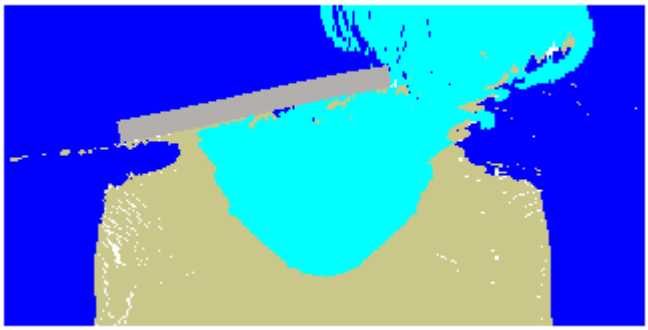

Figure 14. Landmine blast below a steel plate. (Soil1-8ms)

The vertical momentum transferred to the plate when the problem is simulated with different types of soil are represented in Figure 15. Lower values of momentum transfer were obtained for soil1 and soil4 than for soil3. The results for soil1 and soil3 resemble those for dry sand in Gupta (1999) while the results obtained for soil3 are similar to the results for wet sand in Gupta (1999).

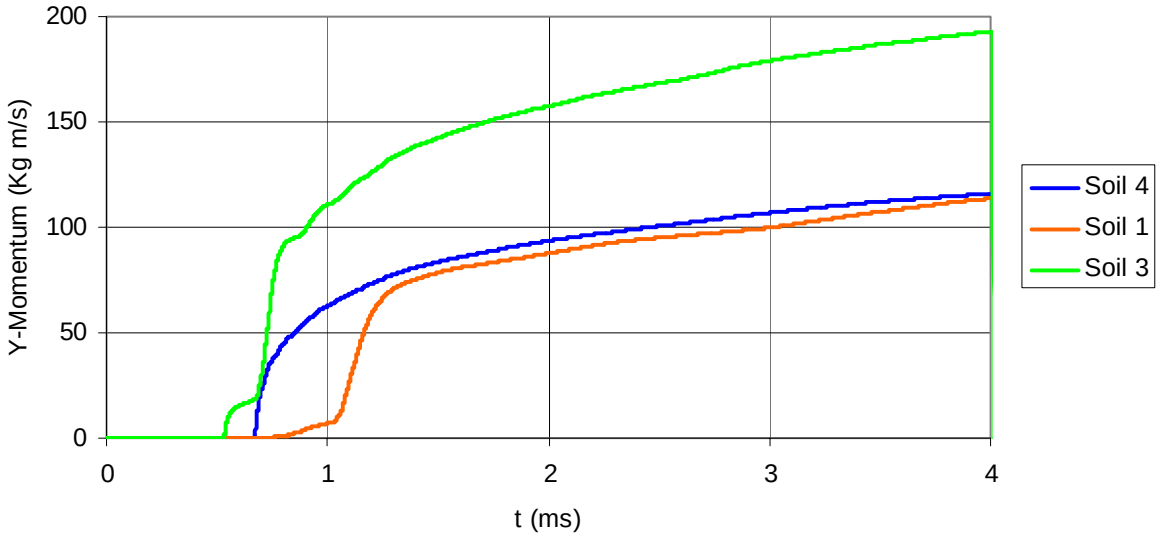

Figure 15. Y-Momentum transfer to the plate for different soil models

In general, higher values of plate rotation than those reported by Gupta (1999) were obtained.

7 CONCLUSIONS

Numerical results for the propagation of blast wave in soils are coincident with those suggested by codes and obtained by other authors. They are strongly dependent on the type of soil modeled. Consequently, in order to assess the effect of buried explosions on underground structures, the soil properties and model should be more carefully studied and defined. For this purpose, underground structures should be explicitly modeled.

The effect of underground explosions on objects placed over the ground level also depends on soil properties. The influence of soil properties is practically negligible for null overburden but increases with the overburden of the explosive load. The results obtained for the soil models analyzed are comparable to experimental results for small overburdens, up to 100mm. Considerable difference between numerical and experimental results is obtained for the highest overburden analyzed. This difference could be attributed not only to the soil model but also to the Euler multi-material processor used for the soil. The Euler processor is not able to reproduce the actual soil ejecta.

Further research, including soil model and processors is needed in the area of underground explosions and their effect on buried and over ground structures. Moreover, experimental results confirm that the degree of saturation of soils and sand plays an important role in its mechanical response during impact/blast loading. Constitutive models for soil should be improved in order to include this variable.

8 AKNOWLEDGEMENTS

The financial support of the CONICET (Argentina) and CIUNT (National University of Tucumán) is gratefully acknowledged.

9 REFERENCES

Alia, A. and Souli, M., High explosive simulation using multi-material formulations. *Applied Thermal Engineering*, 26:1032–1042, 2006

Ambrosini, R.D., Luccioni, B. and Danesi, R., Riera, J. and Rocha, M.. Size of Craters Produced by Explosive Charges on or Above the Ground Surface. *Shock Waves*, 12(1):69-78, 2002.

Ambrosini, R.D., Luccioni, B. and Danesi, R.. Influence of the soil properties on craters produced by explosions on the soil surface. *Computational Mechanics*, XXIII:571-590, 2004.

Ambrosini, R.D. and Luccioni, B. Luccioni. Craters produced by explosions on the soil surface. *Journal of Applied Mechanics, ASME*, 73(6):890-900, 2006

AUTODYN, *Explicit Software for Non-Linear Dynamics*, Version 11.0, User's Manual. Century Dynamics Inc, 2007.

Cendón, D. A. Sánchez Gálvez, V. and Gálvez, F. Modelling explosions using ALE meshes: The influence of mesh refinement in pressures and in efforts induced by blast/structure interaction, *Structures and Materials*, 15:173-180, 2004.

Cheeseman, B.A., Wolf, S., Yen, C.F. and Skaggs, R. Blast simulation of explosives buried in saturated sand. *Fragblast*, 10 (1-2):1-8, 2006.

Elgy, I.D., Pope, D.J. and Pickup, I.M. A study of combined particle and blast wave loading of structures. *Journal De Physique. IV: JP*, 134:467-471, 2006.

Formby, S.A. and Wharton, R.K. Blast characteristics and TNT equivalence values for some commercial explosives detonated at ground level. *Journal of Hazardous Materials,* 50:183-198, 1996.

Grujicic, M, Pandurangan, B., and Cheeseman, B.A. The effect of degree of saturation of sand on detonation phenomena associated with shallow-buried and ground-laid mines. *Shock and Vibration*, 13(1):41-61, 2006.

Grujicic, M., Pandurangan, B., Qiao, R, Cheeseman, B.A., Roy, W.N., Skaggs, R.R. and Gupta, R. Parameterization of the porous-material model for sand with different levels of water saturation, Soil Dynamics and Earthquake Engineering 28:20–35, 2008.

Gupta, A.D. Estimation of vehicle floor plate loading and response due to detonation of a mine shallow-buried in dry sand and wet tuff Tuff. *US Army Ground Vehicle Survivability Symposium*, 1999.

Held, M. Momentum distribution of anti-tank mines, 20th International Symposium on Ballistics, Orlando, 2002a.

Held, M. Calibration tests for blast impulse loads on anti-tank mines. MABS17, Las Vegas, 2002b.

Hlady, S. L. Effect of soil parameters on land mine blast. *18th Military Aspects of Blast and Shock (MABS) Conference*, Germany.2004.

Lee, E.L. and Tarver, C.M. Phenomenological model of shock initiation in heterogeneous explosives. *Physics of Fluids*, 23(12):2362-2372, 1980.

Lu, Y., Wang, Z. and Chong, K. A comparative study of buried structure in soil subjected to blast load using 2D and 3D numerical simulations. *Soil Dynamics and Earthquake Engineering,* 25:275–288, 2005.

Luccioni, B. and Ambrosini, R.D. Craters produced by underground explosions. Computational Mechanics, XXV:1603-1614, 2006.

Luccioni, B. and Ambrosini, R.D. Effect of buried explosions. Computational mechanics, XXVI, 2007.

Swinton, RJ and Bergero, DM. Evaluation of a Silent Killer, the PMN Anti-Personnel Blast Mine. DSTO-TR-1582 , AR-013-112, Technical Report, 2004.

TM5-855-1. Fundamental of protective design for conventional weapons. *US Army Engineer Waterways Experiment Station*, Vicksburg; 1984.

Wang Z, Lu Y. Numerical analysis on dynamic deformation mechanism of soils under blast loading. *Soil Dyn Earthq Eng*;23:705–24, 2003.

Wang Z, Hao H, Lu Y. The three-phase soil model for simulating stress wave propagation due to blast loading. Int J Numer Anal Methods Geomech;28:33–56, 2004.

Wang, Z., Lu, Y., Hao, H. and Chong, K. A full coupled numerical analysis approach for buried structures subjected to subsurface blast. *Computers and Structures*, 83:339–356, 2005.